

## C–H Activation-Enabled Synthesis of A Piperazine-Embedded Azadibenzo[*a,g*]corannulene Analogue

Lin Huang,<sup>a,b,c</sup> Mengyu Qiu,<sup>a,b,c</sup> Zhihao Chang,<sup>a,b,c</sup> Duncan L. Browne,<sup>d</sup> Jianhui Huang\*<sup>a,b,c</sup>

Received 00th January 20xx,  
Accepted 00th January 20xx

DOI: 10.1039/x0xx00000x

A novel piperazine-embedded azadibenzo[*a,g*]corannulene analogue was synthesized by a four-step bottom-up synthesis, including a nucleophilic aromatic substitution ( $S_NAr$ ) and a palladium-catalyzed intramolecular C–H activation arylation as key steps. This intriguing molecule represents the first example of an azacorannulene analogue bearing a piperazine ring on its polycyclic skeleton. X-ray diffraction analysis reveals a  $C_2$ -symmetric deformed bowl-shaped structure and one-dimensional columnar packing through  $\pi$ - $\pi$  interactions with slightly offset centres, attributed to the presence of two  $sp^3$  carbons on its polycyclic core.

### Introduction

Corannulene (**1**), as the smallest curved unit of  $C_{60}$ , has attracted much attention for its unique properties originating from the bowl-shaped structure; such as intermolecular packing,<sup>1</sup> dynamic inversion behaviour,<sup>1</sup> and electron deficiency<sup>2</sup> compared to classical planar poly aromatic hydrocarbons. Remarkable progress has been made in synthesizing this partial fullerene-like structure, from the first synthesis of corannulene in 1966,<sup>3</sup> which required 17 steps and yielded only milligram-scale quantities, to a gram-scale 3-step flash vacuum pyrolysis (FVP) synthesis,<sup>4</sup> and to a kilogram solution-phase synthesis.<sup>5</sup> However, the crucial ring-closure step to impose curvature is currently limited to the FVP method or the use of tetrakis(dibromomethyl)fluoranthene as the substrate.<sup>6</sup> The FVP strategy suffers from several drawbacks:<sup>6a</sup> (1) low yield and small scale preparation, (2) zero functional group tolerance, (3) the requirement for high temperatures, typically above 1000 °C, while synthesizing differently substituted tetrakis(dibromomethyl)fluoranthene derivatives requires substantial effort and exhibits poor functional group tolerance.<sup>7</sup> Very recently, it has been discovered that the curvature of corannulene can also be induced in the solid state through mechanochemical synthesis,<sup>8</sup> offering a potential new method to develop such curved  $\pi$ -conjugated systems.<sup>9</sup> With

regard to the broad application of these curved aromatic hydrocarbons,<sup>10</sup> the design and synthesis of corannulene and corannulene bioisosteres have attracted much attention in molecular design and material sciences. These synthetic challenges hamper the availability of corannulene analogues having one or more heteroatoms incorporated into their

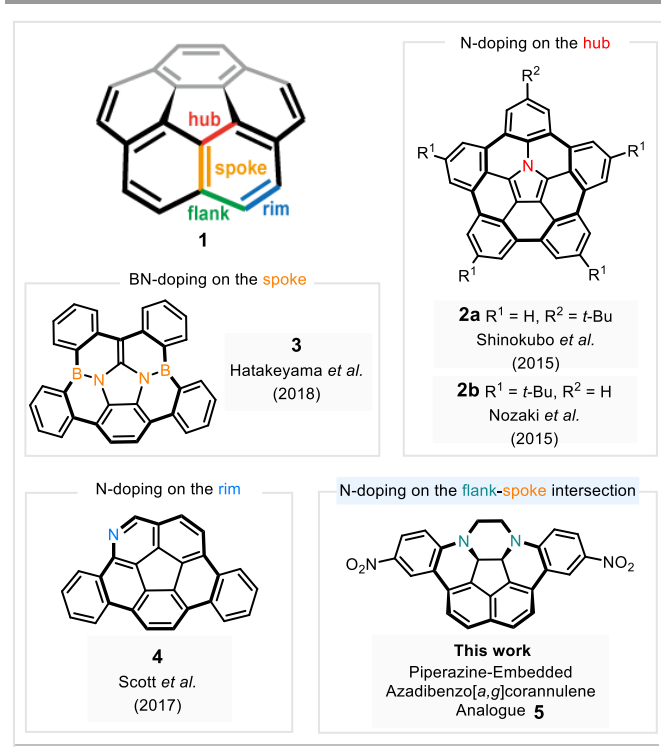


**Fig. 1** Previous reports on heteroatom-incorporated corannulenes within different positions of polycyclic skeleton and our piperazine-embedded azadibenzo[*a,g*]corannulene analogue **5**.

<sup>a</sup> School of Pharmaceutical Science and Technology (SPST), Tianjin University, 92 Weijin Road, Nankai District, Tianjin 300072, P. R. China.

<sup>b</sup> Collaborative Innovation Center of Chemical Science and Engineering, Tianjin 300072, China.

<sup>c</sup> Tianjin Key Laboratory for Modern Drug Delivery & High-Efficiency, Tianjin University, Tianjin 300072, China.

<sup>d</sup> Department of Pharmaceutical and Biological Chemistry, University College London (UCL), School of Pharmacy, 29-39 Brunswick Square, Bloomsbury, London, WC1N 1AX, UK.

† Electronic Supplementary Information (ESI) available: Details of the synthetic procedure and spectroscopic characterization of new compounds, crystallographic data of compounds **5** and **17**. See DOI: 10.1039/x0xx00000x

polycyclic skeletons, there is a need for the development of new bottom-up syntheses. Driven by the strong interest in heteroatom-doped bowl-shaped molecules,<sup>11</sup> several examples of these heteroatom-doped corannulenes have been reported, as shown in Fig. 1. Substituted pentabenzozacorannulenes (**2a**, **2b**) bearing a nitrogen on the hub position of corannulene core;<sup>12</sup> a B<sub>2</sub>N<sub>2</sub>-embedded corannulene **3** in which two C=C units on the spoke of corannulene skeleton were replaced by BN units,<sup>13</sup> and an azacorannulene **4** bearing a nitrogen atom on the rim position,<sup>14</sup> have been synthesized in the last 10 years. However, attempts to synthesize corannulene skeletons with nitrogen atoms embedded on the flank position have not been very successful, possibly because replacing trigonal carbon atoms with trigonal nitrogen atoms leads to the formation of relatively unstable cationic species.<sup>15</sup> The lack of nitrogen atoms embedded on the flank of corannulene core motivated our pursuit of their synthesis. Our recent research interests in transition metal catalyzed C–H direct functionalization<sup>16</sup> have also been focusing on the construction of key C–C bond on curved aromatic systems *via* C–H activation strategies.<sup>17</sup>

Herein, we report the design, synthesis, and X-ray crystallographic analysis of the first piperazine-embedded azadibenzo[*a,g*]corannulene analogue **5** in which two carbon atoms on the flank-spoke intersection of a corannulene skeleton have been replaced with nitrogen atoms. A 4-step bottom-up synthesis from commercially available compounds, including S<sub>N</sub>Ar substitution and a Pd-catalyzed intramolecular C–H activation arylation as key steps, is developed. The formation of by-product **17** during the palladium-catalyzed intramolecular cyclization step indicates an unusual C–N bond cleavage process. The unique analogue **5** is an important precursor to synthesize neutral diazacorannulene and aromatic phenazinium-doped azacorannulene dications.

## Results and discussion

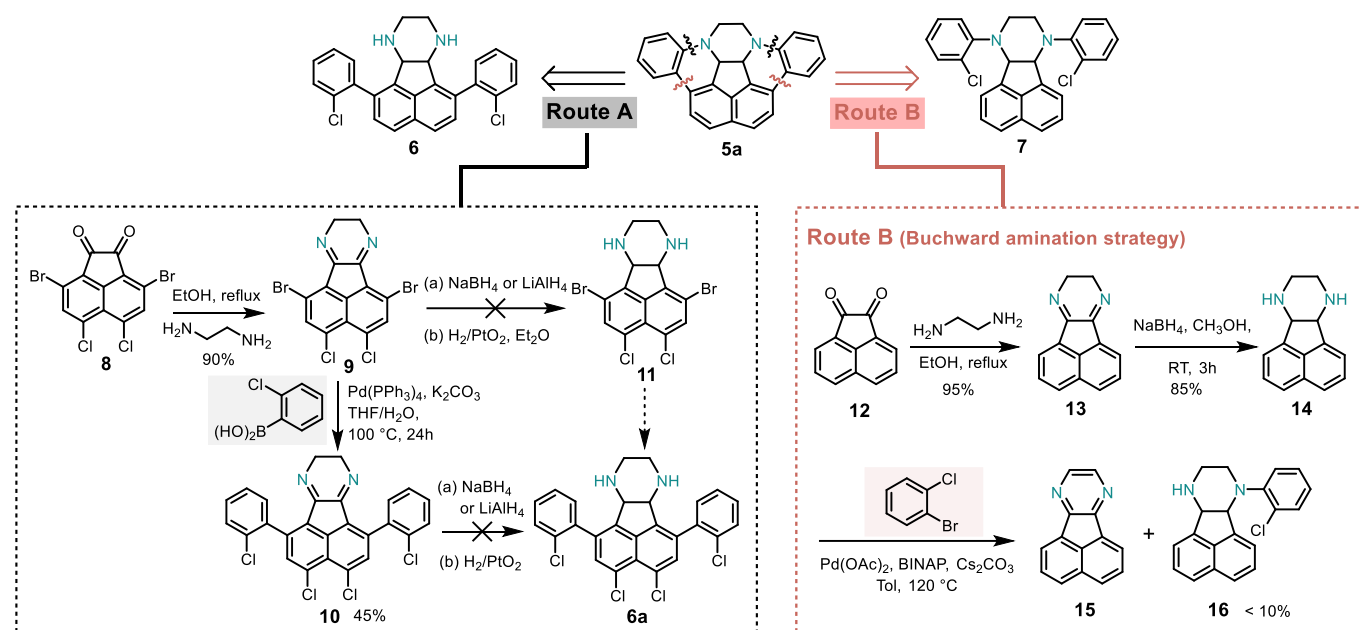
We started our retrosynthetic analysis of piperazine-embedded azadibenzo[*a,g*]corannulene through a Buchwald-Hartwig amination using dichloro acenaphthylene pyrazine **6** as the precursor (Scheme 1, Route A) or a Pd-catalyzed intramolecular C–H activation arylation reaction *via* chloroaryl acenaphthylene pyrazine **7** (Scheme 1, Route B).

Based on our proposals, 3,8-dibromo-5,6-dichloroacenaphthenequinone **8**, prepared from acenaphthene in 3 steps according to Siegel's preparation,<sup>7</sup> was used as the starting material of Route A (Scheme 1, Route A). To introduce nitrogen atoms on the flank position of the corannulene skeleton, diketone **8** underwent a condensation reaction with ethylenediamine in ethanol at reflux, to give dihydropyrazine **9** in 90% yield. However, attempts on the reduction of **9** to **11** all failed in our hands regardless of whether NaBH<sub>4</sub>, LiAlH<sub>4</sub> or H<sub>2</sub>/PtO<sub>2</sub> were employed in the reactions. The failure may be due to the poor solubility of **9** in methanol, THF, and Et<sub>2</sub>O and/or the steric hindrance imparted by the bromine atoms. In a further attempt to elucidate this issue, a Suzuki-Miyaura coupling

reaction between **9** with 2-chlorobenzeneboronic acid was conducted in the presence of Pd(PPh<sub>3</sub>)<sub>4</sub> and K<sub>2</sub>CO<sub>3</sub>, yielding the coupling product **10** with a modest yield of 45%. Despite compound **10** exhibits improved solubility in organic solvents compared to **9**, subsequent attempts to reduce **10** were also unsuccessful, resulting in only dechlorinated analogues of **6a** under H<sub>2</sub>/PtO<sub>2</sub> conditions. Additionally, the presence of β-hydrogens poses a risk of regenerating **10** during the subsequent intramolecular Buchwald-type cyclization *via* β-hydride elimination. Given these challenges, we decide to discontinue further exploration of Route A.

Due to the unsuccessful outcomes of Route A, our focus was shifted to exploring Route B (Scheme 1, Route B). 8,9-Dihydro-acenaphtho[1,2-*b*]pyrazine **13** was readily synthesized by condensation of acenaphthoquinone **12** and ethylenediamine in a high yield of 95%. Following this, compound **13** was efficiently reduced to **14** in the presence of NaBH<sub>4</sub> at room temperature in 85% isolated yield. To synthesize chloroaryl acenaphthylene pyrazine **7** from pyrazine **14**, both Buchwald-Hartwig amination and nucleophilic aromatic substitution (S<sub>N</sub>Ar) strategies were explored. Various conditions within the Buchwald-Hartwig amination were tested, including a range of ligands (dppf, BINAP, Xphos, Ruphos, PPh<sub>3</sub>, P(cy)<sub>3</sub>, P<sup>t</sup>Bu<sub>3</sub>) and bases (NaO<sup>t</sup>Bu, Cs<sub>2</sub>CO<sub>3</sub> and K<sub>2</sub>CO<sub>3</sub>). However, none yielded the targeted product **7** successfully. The most promising results were achieved using Pd(OAc)<sub>2</sub>, Cs<sub>2</sub>CO<sub>3</sub>, and BINAP, with the reaction conducted at 120 °C overnight in toluene under nitrogen atmosphere. Despite these optimized conditions, only a small amount of mono-substituted product **16** (< 10%) was obtained (Scheme 1, Route B Buchwald amination strategy). Additionally, the formation of oxidation side-product acenaphtho[1,2-*b*]pyrazine **15** was formed as the major product, indicating a predominant β-hydride elimination in this Pd-catalyzed reaction, rather than the desired coupling processes.

The unsuccessful coupling reactions using Buchwald amination strategy led us to pivot towards the S<sub>N</sub>Ar strategy, which is widely utilized for the functionalization of (hetero)aromatic systems.<sup>18</sup> Initially, 1-chloro-2-fluorobenzene was chosen as the substrate, aiming to synthesize the disubstituted product **7** using NaH in DMSO or LiHMDS<sup>18d</sup> in THF at 25 °C, though both attempts did not succeed (Table 1, entries 1–2). This underscored the challenges posed by the nucleophile **14**'s low reactivity and propensity for oxidation. Subsequently, 3-chloro-4-fluoronitrobenzene, owing to its higher electrophilicity, was selected as a more promising starting material for reacting with nucleophile **14**. A comprehensive screening of solvents, alongside both organic and inorganic bases, varying equivalents of base and 3-chloro-4-fluoronitrobenzene, and temperatures ranging from 100 to 140 °C, was conducted. Initial efforts using sodium hydride in polar solvents such as DMSO or DMF for deprotonating substrate **14** yielded low amounts of the mono-substituted product **16a**, accompanied by the oxidized



**Scheme 1** Retrosynthetic analysis for piperazine-embedded azadibenzo[*a,g*]corannulene, and exploration of Route A and Route B (Buchwald amination strategy).

**Table 1.** Reaction conditions and isolated yields of  $\text{S}_\text{N}\text{Ar}$ .

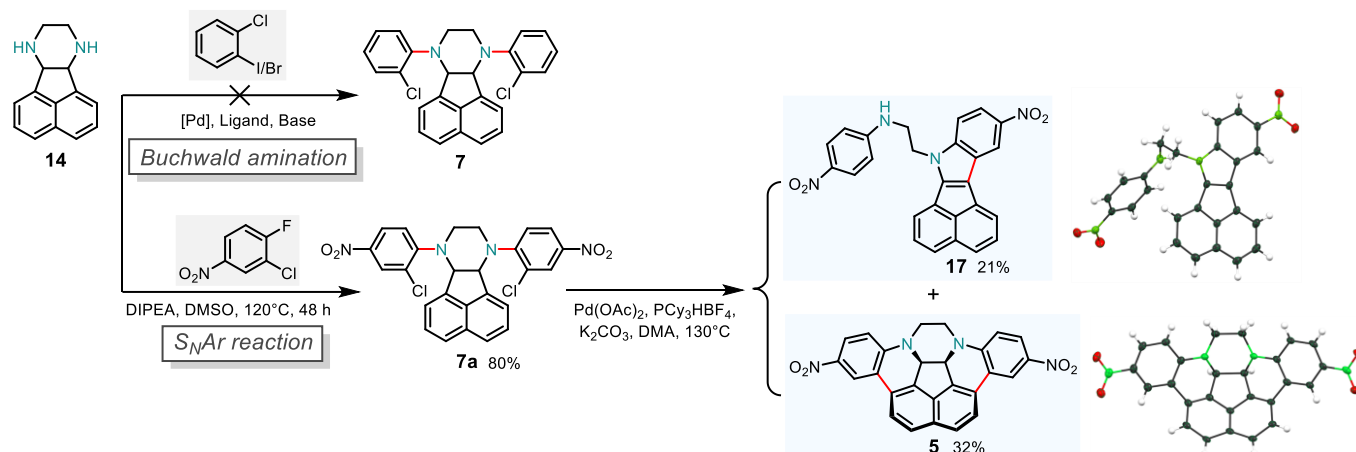
Entry	Base	Solvent <sup>a</sup>	Conditions <sup>b</sup>	Yields <sup>c</sup> (%)		
				15	16a	7a
1 <sup>d</sup>	LiHMDS	THF	25 °C/2 h			N.R.
2 <sup>d</sup>	NaH	DMSO	25 °C/12 h			N.R.
3 <sup>e</sup>	NaH	DMSO	100 °C/24 h	10	25	tr
4 <sup>f</sup>	NaH	DMF	100 °C/24 h	15	30	tr
5 <sup>g</sup>	$\text{K}_2\text{CO}_3$	DMF	100 °C/24 h	5	20	15
6 <sup>h</sup>	$\text{Cs}_2\text{CO}_3$	DMF	100 °C/24 h	20	tr	tr
7 <sup>i</sup>	$\text{K}_2\text{CO}_3$	$\text{CH}_3\text{CN}$	100 °C/24 h	tr	26	tr
8 <sup>j</sup>	DIPEA	DMF	120 °C/24 h	0	17	40
9	DIPEA	THF	120 °C/24 h			N.R.
10	DIPEA	DMF	140 °C/24 h	0	30	60
11	DIPEA	DMSO	120 °C/24 h	0	26	63
12	DIPEA	DMSO	140 °C/24 h	0	35	54
13	DIPEA	DMSO	100 °C/36 h	0	15	60
14 <sup>k</sup>	DIPEA	DMSO	120 °C/24 h	0	40	42
15 <sup>k</sup>	DIPEA	DMSO	120 °C/48 h	0	<5	80

<sup>a</sup>Anhydrous solvents were used. <sup>b</sup>A mixture of pyrazine **14** (0.3 mmol), 3-chloro-4-fluoronitrobenzene (0.9 mmol), base (0.9 mmol), and solvent (1 mL) were heated and stirred under argon atmosphere. <sup>c</sup> Isolated yield. <sup>d</sup> 1-Chloro-2-fluorobenzene (0.9 mmol) was used. <sup>e</sup> ~60% substrate **14** was recovered. <sup>f</sup> ~50% substrate **14** was recovered. <sup>g</sup> ~40% substrate **14** was recovered. <sup>h</sup> ~65% substrate **14** was recovered. <sup>i</sup> ~50% substrate **14** was recovered. <sup>j</sup> ~35% substrate **14** was recovered. <sup>k</sup> DIPEA (1.5 mmol) and 3-chloro-4-fluoronitrobenzene (1.5 mmol) were used. N.R. = No reaction, tr = traces, DIPEA = *N,N*-Diisopropylethylamine.

side-product **15** (Table 1, entries 3–4). Switching from sodium hydride to weaker bases like  $\text{K}_2\text{CO}_3$  and  $\text{Cs}_2\text{CO}_3$  did not alleviate these issues (Table 1, entries 5–6). Gratifyingly, *N,N*-diisopropylethylamine (DIPEA) was found to effectively facilitate this substitution (Table 1, entry 8). The solvent DMSO was also identified as critical for success, with alternatives like THF and  $\text{CH}_3\text{CN}$  failing to produce the desired product **7a** (Table 1, entries 7 and 9). This led to a focused exploration of reaction conditions using DMSO and DIPEA, optimizing temperature, reaction time, and substrate ratios (Table 1, entries 11–15). The optimal conditions involved treating **14** with five equivalents each of DIPEA and 3-chloro-4-fluoronitrobenzene at 120 °C for 48 hours, achieving an isolated yield of up to 80% for precursor **7a** (Table 1, entry 15). This yield presents a viable route for scaling up and lays a strong groundwork for the next phase of ring-closure step.

Transition metal-catalyzed coupling reactions, through HX eliminations (where X = Cl, Br, OTf, etc.),<sup>19</sup> have been established as valuable methods for synthesizing non-planar carbocycles,<sup>20</sup> heterocycles,<sup>21</sup> and various natural products.<sup>22</sup> Based on our continuous research interests in Pd-catalyzed C–H activation cyclization reactions,<sup>16–17</sup> and with precursor **7a** ready, we initiated the screening of reaction conditions. Fortunately, the piperazine-embedded azadibenzo[*a,g*]corannulene analogue **5** was successfully obtained by the treatment of **7a** with excess  $\text{K}_2\text{CO}_3$ ,  $\text{Pd}(\text{OAc})_2$ , and  $\text{PCy}_3\text{HBF}_4$  in dry DMA under  $\text{N}_2$  atmosphere at 130 °C for 24 hours, although with an unexpected by-product **17**, as shown in Scheme 2.

## ARTICLE



**Scheme 2.** The synthetic route to piperazine-embedded azadibenzo[*a,g*]corannulene analogue **5** and unexpected by-product **17** via Pd-catalyzed C–H activation cyclization and their crystal structures.

The structures of both **5** and **17** were confirmed by nuclear magnetic resonance (NMR) spectroscopy, high-resolution mass spectrometry (HRMS), and X-ray diffraction analysis. The  $^1\text{H}$  NMR spectrum of **5** in  $\text{DMSO-}d_6$  revealed the presence of five different aromatic proton environments: four doublets and one doublet of doublets, and two aliphatic proton environments: one singlet and one multiplet, thus indicating that **5** possesses  $C_s$  symmetry. The HRMS of **5** exhibited an  $m/z$  value of 449.1246, which corresponds to an ion mass of  $\text{C}_{26}\text{H}_{17}\text{N}_4\text{O}_4$  ( $m/z$ : 449.1250). The obtained **5** has a poor solubility in various organic solvents, which causes significant difficulties during the isolation and purification process. The azacorannulene analogue **5** is also found to be unstable under ambient air conditions and undergoes degradation within a few weeks. This instability is likely attributed to the distorted structure, which renders the lone pair of electrons on the nitrogen atoms susceptible to oxidation by air.

Despite the unstable nature of this azacorannulene precursor **5**, single crystals suitable for X-ray diffraction analysis were obtained by slow evaporation of dichloromethane solution of **5** at room temperature. The X-ray crystallographic analysis, as shown in Fig. 2, revealed a  $C_s$ -symmetrical deformed bowl-shaped structure attributed to the two  $\text{sp}^3$ -carbon atoms (C20, C21). The bowl depths, defined as the perpendicular distance from the center of the hub ring (Fig. 2A, ring C) to the parallel planes containing carbon atoms C10/C12, C9/C13, C3/C14, C15/C22 and nitrogen atoms N1/N2, are 0.55, 0.71, 1.13, 1.49 and 1.17 Å (Fig. 2B), respectively. The bowl depth, as measured at rings B and D that contain the  $\text{sp}^3$ -carbon atoms, ranges from

1.13 to 1.49 Å, which is greater than that of pristine corannulene (0.87 Å),<sup>23</sup> indicating the influence of two  $\text{sp}^3$ -carbon atoms (C20, C21) on the deformed bowl-shaped structure. The deformed non-planar naphthalene ring (rings E and F), as shown in Fig. 2A and B, exhibits a bowl depth of

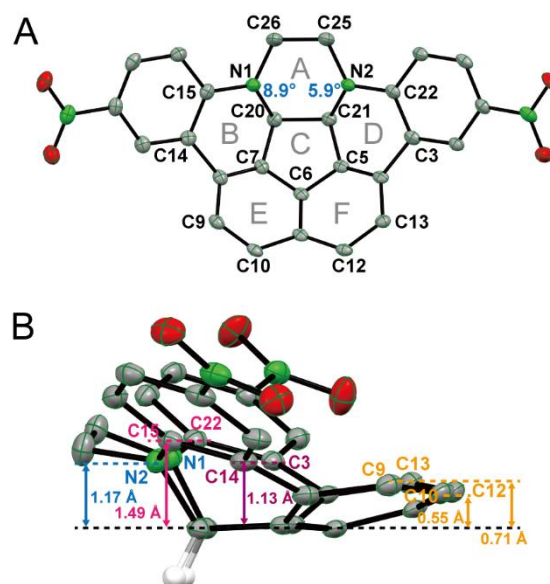


**Fig. 2** Structural features of azacorannulene analogue **5**. (A) Top view and POAV pyramidalization angles, (B) side view and bowl depth. Thermal ellipsoids are scaled at 50% probability level and partial hydrogen atoms are omitted for clarity.

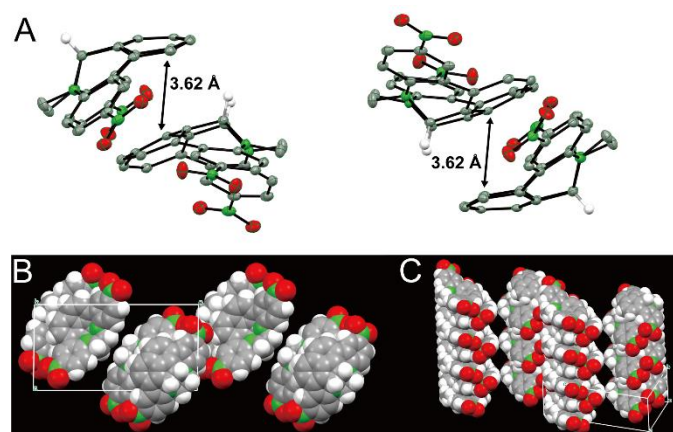


**Fig. 3. Crystal packing.** (A) packing structure in the crystal. Thermal ellipsoids are scaled at 50% probability level and partial hydrogen atoms are omitted for clarity. (B) Crystal packing structures of **5** along *b* axis. (C) Columnar packing.

0.55–0.71 Å, which is smaller than corannulene (0.87 Å),<sup>23</sup> suggesting a reduced strain in **5** upon the introduction of a piperazine ring into the corannulene skeleton. The tertiary N1 and N2 exhibit  $\pi$ -orbital axis vector (POAV) angles<sup>24</sup> of 8.9° and 5.9° (Fig. 2A), respectively, indicating a nearly planar structure, which gives them partial  $sp^2$  hybridization characteristics. This could be attributed as a reason why piperazine-embedded azadibenzo[*a,g*]corannulene analogue **5** is sensitive to air atmosphere. As shown in Fig. 3, **5** exhibits a one-directional *concave-to-convex*  $\pi$ -stacking structure along the *b* axis with the centres slightly offset from each other,<sup>1b, 1d</sup> because of the deformed-bowl structure. The stacking distance is 3.62 Å (Fig. 3A), which is slightly smaller than that of sumanene (3.86 Å),<sup>25</sup> a  $C_{3v}$ -symmetric bowl-shaped polycyclic aromatic molecule.

Interestingly, the by-product **17**, which is further confirmed by X-ray crystallography, is significantly different from the cyclization product **5**. The proposed mechanism involves an unexpected C–N bond cleavage process, as shown in Fig. 4. It initiates with the oxidative addition (OA<sup>1</sup>) of palladium(0) to a C–Cl bond in compound **7a**, leading to the formation of the organopalladium intermediate **A**. The next C–H activation step could be divided into two pathways depending on the hydrogen involved. The first pathway involves the activation of hydrogen (OA) on the naphthalene ring (colored in red), forming a seven-membered metallacycle intermediate **G**, followed a reductive elimination step. This process is then repeated once, ultimately leading to the target **5**. The second pathway is more complex. It begins with the activation (OA<sup>2</sup>) of a benzyl hydrogen (colored in blue), leading to a five-membered metallacycle intermediate **B**. Subsequently, reductive elimination (RE<sup>1</sup>) and  $\beta$ -hydride elimination steps result in intermediate **D**. Then, intermediate **D** undergoes oxidative addition (OA<sup>3</sup>) to the remaining C–Cl bond, followed by a C–N bond insertion process (OA<sup>4</sup>), which is facilitated by coordination with the formed C=C bond, leading to intermediate **F**. This step is crucial for the formation of by-

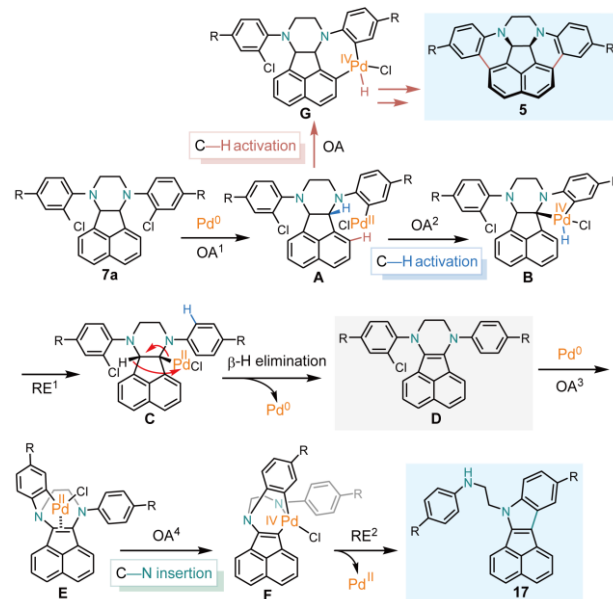


**Fig. 4** Proposed mechanism. (R = NO<sub>2</sub>; OA = oxidative addition; RE = reductive elimination).

product **17**. Finally, **17** is obtained through a further reductive elimination (RE) step. The proposed mechanism involves two key steps: the activation of a different hydrogen and the palladium insertion into the C–N bond. Both these processes determine the ratio of the target product **5** and by-product **17**.

Due to the incorporation of a piperazine ring into the flank of corannulene skeleton, which includes  $sp^3$  carbons, the aromaticity of analogue **5** is disrupted. This makes the oxidation of precursor **5** to form cationic aromatic azacorannulene derivatives of significant interest.<sup>26</sup> Further research to synthesize those aromatic azacorannulene salts from piperazine-embedded azadibenzo[*a,g*]corannulene analogue **5** is currently underway in our laboratory.

## Conclusions

In summary, we report the first bottom-up synthesis of piperazine-embedded azadibenzo[*a,g*]corannulene analogue **5**, including a nucleophilic aromatic substitution ( $S_NAr$ ) and a palladium-catalyzed intramolecular C–H activation arylation as key steps. This intriguing molecule was fully characterized by NMR spectroscopy, HRMS, and X-ray diffraction analysis. Single crystal X-ray analysis reveals a  $C_s$  symmetric deformed bowl-shaped structure and one-dimensional columnar packing through  $\pi$ - $\pi$  interactions with slightly offset centres. The formation of by-product **17** during the Pd-catalyzed intramolecular cyclization step involves an unusual C–N bond cleavage process. This work not only introduces a promising precursor but also offers valuable insights for developing new strategies to synthesize curved azaaromatic compounds.

## Author Contributions



L. H. & J. H. conceptualized the study. L. H. & M. Q. performed the experiments and data analysis. Z. C. helped with the synthetic experiments. L. H. wrote original manuscript. D. L. B. & J. H. revised and edited the manuscript. J. H. acquired funding and supervised the project. All authors have given approval to the final version of the manuscript.

### Conflicts of interest

There are no conflicts to declare.

### Acknowledgements

The authors are grateful for the funding support from National Program on Key Basic Research Project of China (973 Program) (2015CB856500) and National Natural Science Foundation of China (NSFC) (grant number 21672159 and 21871207). The Instrumental Analysis Center of SPST at Tianjin University is acknowledged for providing NMR, HRMS, and X-ray crystal diffraction analysis. The authors thank Dr. Jun Xu for assistance with single crystal analysis, and also Dr. Yan Guo for assistance with the HRMS analysis. The authors are further thankful to Jay S. Siegel for the constructive comments and suggestions.

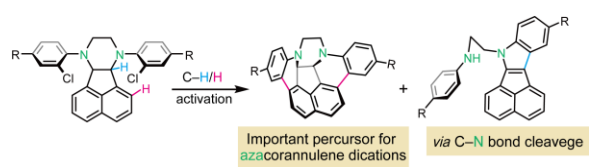
### Notes and references

- (a) J. C. Hanson; C. E. Nordman. The Crystal and Molecular Structure of Corannulene, C<sub>20</sub>H<sub>10</sub>. *Acta Cryst. B* 1976, **32**, 1147–1153. (b) Y. T. Wu; D. Bandera; R. Maag; A. Linden; K. K. Baldrige; J. S. Siegel. Multiethynyl Corannulenes: Synthesis, Structure, and Properties. *J. Am. Chem. Soc.* 2008, **130**, 10729–10739. (c) T. Guo; A. Li; J. Xu; K. K. Baldrige; J. S. Siegel. Enantiopure C<sub>5</sub> Pentaindenocorannulenes: Chiral Graphenoid Materials. *Angew. Chem. Int. Ed.* 2021, **60**, 25809–25814. (d) Q. Q. Li; Y. Hamamoto; G. Kwek; B. Xing; Y. Li; S. Ito. Diazapentabenzocorannulenium: A Hydrophilic/Biophilic Cationic Buckybowl. *Angew. Chem. Int. Ed.* 2022, **61**, e202112638.
- (a) A. Borchardt; A. Fuchicello; K. V. Kilway; K. K. Baldrige; J. S. Siegel. Synthesis and Dynamics of the Corannulene Nucleus. *J. Am. Chem. Soc.* 1992, **114**, 1921–1923. (b) L. T. H. Scott, Mohammed M. Bratcher, Matthew S. Corannulene Bowl-to-Bowl Inversion is Rapid at Room Temperature. *J. Am. Chem. Soc.* 1992, **114**, 1920–1921. (c) T. J. Seiders; K. K. Baldrige; G. H. Grube; J. S. Siegel. Structure/Energy Correlation of Bowl Depth and Inversion Barrier in Corannulene Derivatives: Combined Experimental and Quantum Mechanical Analysis. *J. Am. Chem. Soc.* 2001, **123**, 517–525. (d) M. Juriček; N. L. Strutt; J. C. Barnes; A. M. Butterfield; E. J. Dale; K. K. Baldrige; J. F. Stoddart; J. S. Siegel. Induced-Fit Catalysis of Corannulene Bowl-to-Bowl Inversion. *Nat. Chem.* 2014, **6**, 222–228.
- (a) A. Ayalon; M. Rabinovitz; P.-C. Cheng; L. T. Scott. Corannulene Tetraanion: A Novel Species with Concentric Anionic Rings. *Angew. Chem. Int. Ed.* 1992, **31**, 1636–1637. (b) A. Ayalon; A. Sygula; P.-C. Cheng; M. Rabinovitz; P. W. Rabideau; L. T. Scott. Stable High-Order Molecular Sandwiches: Hydrocarbon Polyanion Pairs with Multiple Lithium Ions Inside and Out. *Science* 1994, **265**, 1065–1067. (c) A. V. Zabula; A. S. Filatov; S. N. Spisak; A. Y. Rogachev; M. A. Petrukhina. A Main Group Metal Sandwich: Five Lithium Cations Jammed between Two Corannulene Tetraanion Decks. *Science* 2011, **333**, 1008–1011.
- W. E. Barth; R. G. Lawton. Dibenzo[ghi,mno]fluoranthene. *J. Am. Chem. Soc.* 1966, **88**, 380–381.
- (a) L. T. Scott; M. M. Hashemi; D. T. Meyer; H. B. Warren. Corannulene. A Convenient New Synthesis. *J. Am. Chem. Soc.* 1991, **113**, 7082–7084. (b) L. T. Scott; P.-C. Cheng; M. M. Hashemi; M. S. Bratcher; D. T. Meyer; H. B. Warren. Corannulene. A Three-Step Synthesis. *J. Am. Chem. Soc.* 1997, **119**, 10963–10968.
- A. M. Butterfield; B. Gilomen; J. S. Siegel. Kilogram-Scale Production of Corannulene. *Org. Process Res. Dev.* 2012, **16**, 664–676.
- (a) V. M. Tsefrikas; L. T. Scott. Geodesic Polyarenes by Flash Vacuum Pyrolysis. *Chem. Rev.* 2006, **106**, 4868–4884. (b) Y.-T. Wu; J. S. Siegel. Aromatic Molecular-Bowl Hydrocarbons: Synthetic Derivatives, Their Structures, and Physical Properties. *Chem. Rev.* 2006, **106**, 4843–4867.
- T. J. Seiders; E. L. Elliott; G. H. Grube; J. S. Siegel. Synthesis of Corannulene and Alkyl Derivatives of Corannulene. *J. Am. Chem. Soc.* 1999, **121**, 7804–7813.
- (a) G. Băti; S. Laxmi; M. C. Stuparu. Mechanochemical Synthesis of Corannulene: Scalable and Efficient Preparation of a Curved Polycyclic Aromatic Hydrocarbon under Ball Milling Conditions. *ChemSusChem* 2023, **16**, e202301087. (b) T. Yong; G. Băti; F. García; M. C. Stuparu. Mechanochemical Transformation of Planar Polyarenes to Curved Fused-Ring Systems. *Nat. Commun.* 2021, **12**, 5187.
- (a) G. Băti; D. Csókás; T. Yong; S. M. Tam; R. R. S. Shi; R. D. Webster; I. Pápai; F. García; M. C. Stuparu. Mechanochemical Synthesis of Corannulene-Based Curved Nanographenes. *Angew. Chem. Int. Ed.* 2020, **59**, 21620–21626. (b) J. Stanojkovic; R. William; Z. Zhang; I. Fernández; J. Zhou; R. D. Webster; M. C. Stuparu. Synthesis of Precisely Functionalizable Curved Nanographenes Via Graphitization-Induced Regioselective Chlorination in a Mechanochemical Scholl Reaction. *Nat. Commun.* 2023, **14**, 803.
- (a) E. Nestoros; M. C. Stuparu. Corannulene: A Molecular Bowl of Carbon with Multifaceted Properties and Diverse Applications. *Chem. Commun.* 2018, **54**, 6503–6519. (b) M. C. Stuparu. Corannulene: A Curved Polyarene Building Block for the Construction of Functional Materials. *Acc. Chem. Res.* 2021, **54**, 2858–2870.
- (a) M. Stępień; E. Gońka; M. Żyła; N. Sprutta. Heterocyclic Nanographenes and Other Polycyclic Heteroaromatic Compounds: Synthetic Routes, Properties, and Applications. *Chem. Rev.* 2017, **117**, 3479–3716. (b) A. Borissov; Y. K. Maurya; L. Moshniaha; W.-S. Wong; M. Żyła-Karwowska; M. Stępień. Recent Advances in Heterocyclic Nanographenes and Other Polycyclic Heteroaromatic Compounds. *Chem. Rev.* 2021, **122**, 565–788. (c) T. Tanaka; K. Kise. Non-Planar Polycyclic Aromatic Molecules Including Heterole Units. *Heterocycles* 2022, **104**, 1373. (d) M. Saito; H. Shinokubo; H. Sakurai. Figuration of Bowl-Shaped  $\pi$ -Conjugated Molecules: Properties and Functions. *Mater. Chem. Front.* 2018, **2**, 635–661.
- (a) S. Ito; Y. Tokimaru; K. Nozaki. Benzene-Fused Azacorannulene Bearing an Internal Nitrogen Atom. *Angew. Chem. Int. Ed.* 2015, **54**, 7256–7260. (b) H. Yokoi; Y. Hiraoka; S. Hiroto; D. Sakamaki; S. Seki; H. Shinokubo. Nitrogen-Embedded Buckybowl and Its Assembly with C<sub>60</sub>. *Nat. Commun.* 2015, **6**, 8215.
- S. Nakatsuka; N. Yasuda; T. Hatakeyama. Four-Step Synthesis of B<sub>2</sub>N<sub>2</sub>-Embedded Corannulene. *J. Am. Chem. Soc.* 2018, **140**, 13562–13565.
- V. M. Tsefrikas; A. K. Greene; L. T. Scott. 5-Azadibenzo[a,g]corannulene. *Org. Chem. Front.* 2017, **4**, 688–698.
- (a) J. Nagasaki; S. Hiroto; H. Shinokubo.  $\pi$ -Extended Dihydrophenazines with Three-State NIR Electrochromism

- Involving Large Conformational Changes. *Chem. – Asian J.* 2017, **12**, 2311–2317. (b) J. Dosso; B. Bartolomei; N. Demitri; F. P. Cossío; M. Prato. Phenanthrene-Extended Phenazine Dication: An Electrochromic Conformational Switch Presenting Dual Reactivity. *J. Am. Chem. Soc.* 2022, **144**, 7295–7301.
- 17 (a) H. Zhong; D. Yang; S. Wang; J. Huang. Pd-Catalysed Synthesis of Isoquinolinones and Analogues via C–H and N–H Bonds Double Activation. *Chem. Commun.* 2012, **48**, 3236–3238. (b) W. Liu; Q. Yu; L. Hu; Z. Chen; J. Huang. Modular Synthesis of Dihydro-isoquinolines: Palladium-Catalyzed Sequential C(Sp<sup>2</sup>)-H and C(Sp<sup>3</sup>)-H Bond Activation. *Chem. Sci.* 2015, **6**, 5768–5772. (c) Q. Yu; L. a. Hu; Y. Wang; S. Zheng; J. Huang. Directed meta-Selective Bromination of Arenes with Ruthenium Catalysts. *Angew. Chem. Int. Ed.* 2015, **54**, 15284–15288. (d) Z. Chen; L. Hu; F. Zeng; R. Zhu; S. Zheng; Q. Yu; J. Huang. Selective mono-Alkylation of N-Methoxybenzamides. *Chem. Commun.* 2017, **53**, 4258–4261. (e) Y. Wang; J. Liu; L. Huang; R. Zhu; X. Huang; R. Moir; J. Huang. KO<sup>t</sup>Bu-Catalyzed Lithiation of PMDTA and the Direct Functionalization of Bridged Alkenes under Mild Conditions. *Chem. Commun.* 2017, **53**, 4589–4592. (f) Q. Wang; X. Fu; Y. Yan; T. Liu; Y. Xie; X. Song; Y. Zhou; M. Xu; P. Wang; P. Fu; J. Huang; N. Huang. Structure-Based Identification of Organoruthenium Compounds as Nanomolar Antagonists of Cannabinoid Receptors. *J. Chem. Inf. Model.* 2024, **64**, 761–774.
- 18 L. Huang; Q. Wang; P. Fu; Y. Sun; J. Xu; L. D. Browne; J. Huang. Extended Quinolizinium-Fused Corannulene Derivatives: Synthesis and Properties. *JACS Au* 2024, DOI: org/10.1021/jacsau.4c00105.
- 19 (a) P. S. Fier; J. F. Hartwig. Synthesis and Late-Stage Functionalization of Complex Molecules through C–H Fluorination and Nucleophilic Aromatic Substitution. *J. Am. Chem. Soc.* 2014, **136**, 10139–10147. (b) C. N. Neumann; J. M. Hooker; T. Ritter. Concerted Nucleophilic Aromatic Substitution with <sup>19</sup>F<sup>-</sup> and <sup>18</sup>F<sup>-</sup>. *Nature* 2016, **534**, 369–373. (c) F. Diness; D. P. Fairlie. Catalyst-Free N-Arylation Using Unactivated Fluorobenzenes. *Angew. Chem. Int. Ed.* 2012, **51**, 8012–8016. (d) C. B. Jacobsen; M. Meldal; F. Diness. Mechanism and Scope of Base-Controlled Catalyst-Free N-Arylation of Amines with Unactivated Fluorobenzenes. *Chem. – Eur. J.* 2016, **23**, 846–851.
- 20 (a) Y. Yu; U. K. Tambar. Palladium-Catalyzed Cross-Coupling of  $\alpha$ -Bromocarbonyls and Allylic Alcohols for the Synthesis of  $\alpha$ -Aryl Dicarbonyl Compounds. *Chem. Sci.* 2015, **6**, 2777–2781. (b) B. Xu; U. K. Tambar. Remote Allylation of Unactivated C(Sp<sup>3</sup>)-H Bonds Triggered by Photogenerated Amidyl Radicals. *ACS Catal.* 2019, **9**, 4627–4631.
- 21 (a) H.-I. Chang; H.-T. Huang; C.-H. Huang; M.-Y. Kuo; Y.-T. Wu. Diindeno[1,2,3,4-defg;1',2',3',4'-mnop]chrysenes: Solution-Phase Synthesis and the Bowl-to-Bowl Inversion Barrier. *Chem. Commun.* 2010, **46**, 7241–7243. (b) L. Wang; P. B. Shevlin. Palladium-Mediated Formation of Bowl-Shaped PAHs: Synthesis of as-Indaceno[3,2,1,8,7,6,-pqrstuv]picenes. *Org. Lett.* 2000, **2**, 3703–3705. (c) T.-C. Wu; H.-J. Hsin; M.-Y. Kuo; C.-H. Li; Y.-T. Wu. Synthesis and Structural Analysis of a Highly Curved Buckybowl Containing Corannulene and Sumanene Fragments. *J. Am. Chem. Soc.* 2011, **133**, 16319–16321. (d) H. A. Reisch; M. S. Bratcher; L. T. Scott. Imposing Curvature on a Polyarene by Intramolecular Palladium-Catalyzed Arylation Reactions: A Simple Synthesis of Dibenzo[a,g]corannulene. *Org. Lett.* 2000, **2**, 1427–1430.
- 22 (a) L. Zhou; G. Zhang. A Nanoboat with Fused Concave N-Heterotriangulene. *Angew. Chem. Int. Ed.* 2020, **59**, 8963–8968. (b) Y. Tokimaru; S. Ito; K. Nozaki. A Hybrid of Corannulene and Azacorannulene: Synthesis of a Highly Curved Nitrogen-Containing Buckybowl. *Angew. Chem. Int. Ed.* 2018, **57**, 9818–9822. (c) J. Huang; B. Li; P. Jiao; H. Zhong. Isoquinoline N-Oxide Synthesis under Pd-Catalysed C–H Activation/Annulation Processes. *Synlett* 2013, **24**, 2431–2436. (d) S. Huang; M. Wang; X. Jiang. Ni-Catalyzed C–S Bond Construction and Cleavage. *Chem. Soc. Rev.* 2022, **51**, 8351–8377. (e) F. Richard; P. Clark; A. Hannam; T. Keenan; A. Jean; S. Arseniyadis. Pd-Catalysed Asymmetric Allylic Alkylation of Heterocycles: A User's Guide. *Chem. Soc. Rev.* 2024, **53**, 1936–1983. (f) Q. Lu; S. Mondal; S. Cembellin; S. Greßies; F. Glorius. Site-Selective C–H Activation and Regiospecific Annulation Using Propargylic Carbonates. *Chem. Sci.* 2019, **10**, 6560–6564.
- 23 J. Yamaguchi; A. D. Yamaguchi; K. Itami. C–H Bond Functionalization: Emerging Synthetic Tools for Natural Products and Pharmaceuticals. *Angew. Chem. Int. Ed.* 2012, **51**, 8960–9009.
- 24 R. C. Haddon. Chemistry of the Fullerenes: The Manifestation of Strain in a Class of Continuous Aromatic Molecules. *Science* 1993, **261**, 1545–1550.
- 25 H. Sakurai; T. Daiko; H. Sakane; T. Amaya; T. Hirao. Structural Elucidation of Sumanene and Generation of Its Benzylic Anions. *J. Am. Chem. Soc.* 2005, **127**, 11580–11581.
- 26 (a) R. Berger; A. Giannakopoulos; P. Ravat; M. Wagner; D. Beljonne; X. Feng; K. Müllen. Synthesis of Nitrogen-Doped Zigzag-Edge Peripheries: Dibenzo-9a-azaphenylene as Repeating Unit. *Angew. Chem. Int. Ed.* 2014, **53**, 10520–10524. (b) X.-Y. Wang; M. Richter; Y. He; J. Björk; A. Riss; R. Rajesh; M. Garnica; F. Hennesdorf; J. J. Weigand; A. Narita; R. Berger; X. Feng; W. Auwärter; J. V. Barth; C.-A. Palma; K. Müllen. Exploration of Pyrazine-Embedded Antiaromatic Polycyclic Hydrocarbons Generated by Solution and on-Surface Azomethine Ylide Homocoupling. *Nat. Commun.* 2017, **8**, 1948.

## ARTICLE

## Entry for the Table of Contents



The first azadibenzo[*α,g*]corannulene analogue with a piperazine ring on the flank of its polycyclic skeleton is reported. The synthesis involves a convenient four-step, bottom-up approach that culminates in a Pd-catalyzed C-H activation arylation for final ring closure.